2016 IEEE/RSJ International Conference on Intelligent Robots and Systems (IROS)
Daejeon Convention Center
October 9-14, 2016, Daejeon, Korea

Generalized Information Filtering for MAV Parameter Estimation

Michael Burri, Michael Bloesch, Dominik Schindler, Igor Gilitschenski, Zachary Taylor, Roland Siegwart
Autonomous Systems Lab, ETH Zürich, Switzerland, burrimi@ethz.ch

***Abstract*— In this paper we present a new estimation algorithm that allows for the combination of information from any number of process and measurement models. This adds more flexibility to the design of the estimator and in our case avoids the need for state augmentation. We achieve this by adapting the maximum likelihood formulation of the Kalman Filter, and thereby represent all measurement models as residuals. Posing the problem in this form allows for the straightforward integration of any number of (nonlinear) constraints between two subsequent states. To solve the optimization we present a closed form recursive set of equations that directly marginalizes out information that is not required, this leads to an efficient and generic implementation. The new algorithm is applied to parameter estimation on MAVs which have two dynamic models, the MAV dynamic model and the IMU-driven model. We show the benefits and limitations of the new filtering approach on a simplified simulation example and on a real MAV system.**

I. Introduction

In order to perform the challenging tasks demanded by modern robotic systems, precise estimation of the state and a large number of parameters is required. To allow the estimation of the current state and parameters these systems are equipped with a large array of sensors. However, to make efficient use of all the information provided by these sensors sophisticated sensor fusion algorithms are required.

Modern schemes that perform this parameter estimation tend to utilize a batch optimization process. This provides an accurate maximum likelihood solution for the parameters and allows for the formulation of any residual between multiple states. However, batch optimization can take substantial time to process and generally assumes that the parameter values are constant for the entire dataset. In many situations, the batch processing of data limits the applicability of the approach and an iterative scheme that can provide real-time estimation of dynamic parameters is preferable.

As an example, consider the rapidly growing field of micro aerial vehicles (MAVs). These systems require the estimation of a large number of system parameters including the current pose of the system. This estimation is further complicated for activities such as the transportation of goods, where many of the parameters (mass, mass distribution, inertia, etc) cannot be assumed to be constant values. These systems may also physically interact with the world, in which case the external forces acting on the system must also be estimated in real-time.

This research was supported in part by the European Community's Seventh Framework Programme (grant number n.608849), the Swiss National Science Foundation (SNF) through project 200021_149427/1 and the National Centre of Competence in Research Robotics.

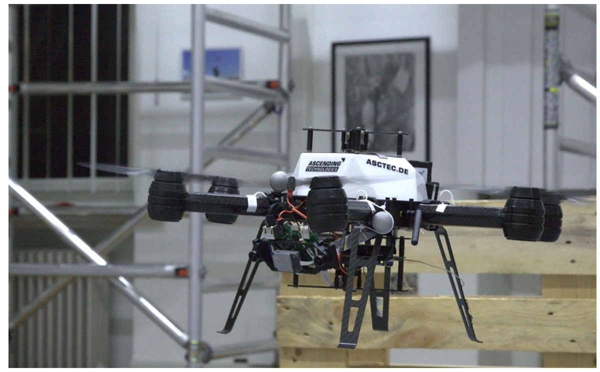

Fig. 1. Image of the MAV used in our parameter estimation experiments.

The influence these parameters have on the system can be observed through the MAV's IMU, dynamic model and any odometry sensors present. Issues arise with this estimation however, as in this situation the MAV possesses two process models (in contrast to an update model, a process model involves two subsequent states). One driven by the IMU and a second based on the dynamic model of the MAV. Situations such as this where multiple models and information sources are present, pose a significant challenge for traditional filters. These difficulties are further complicated when measurement noise and process noise are correlated.

In this case, one could add the IMU to the update step of the filter. However, this would mean augmenting the state vector with the acceleration, which can be challenging to derive an appropriate propagation model for and increases the state vector. In this paper we present a generalized filtering algorithm (GIF), that can overcome this problem and take all the available information into account. It does this without increasing the state vector more than is necessary and without making additional assumptions, such as constant acceleration for the augmented state.

The contributions of this work are:

- We present a generic and flexible filtering algorithm which can handle an arbitrary number of process and measurement models in a computationally efficient way.
- The new algorithm is validated on a simplified simulation example and on experimental data recorded from multiple flights with our MAV.

The remainder of this paper is organized as follows: in Section III, we derive the new filter and show how to apply it to the problem of parameter estimation in Section IV. Finally, we show experimental results in Section V, both on a simplified 1D simulation and on real flight data.

978-1-5090-3762-9/16/$31.00 ©2016 IEEE

II. Related Work

While the original Kalman Filter (KF) [1] and EKF [2] were formulated with one process model in mind, the formulation has been extended to allow the use of multiple models in several different contexts. Interacting Multiple Model (IMM) based filters [3] consider the use of several system models. In this formulation only one model is considered valid at a given timestep. This is in contrast to our approach which can consider multiple models simultaneously.

A similar problem has been considered in the research area of Track-to-Track Fusion (T2TF) [4], [5], [6], which aims at combining locally computed estimates from different sensors. When heterogeneous sensors are involved, this may require different state representations and therefore also differing system models within the individual sensors. This was considered in [7]. One of the main focuses within the T2TF literature, however, is the handling of correlated process noise in decentralized filters. This problem does not arise in our scenario as we are considering a centralized setting.

Simultaneous consideration of multiple process models can be reformulated as one implicit process model. In [8], an implicit model is considered in the prediction step. On the other hand, use of implicit update model equations is discussed in [9]. In this paper we derive a more general formulation unifying both aspects in an information form filter.

Early work on real time parameter estimation on MAVs was done in the frequency domain [10]. By only considering the frequency band of interest it is computationally very efficient and automatically rejects noise in other parts of the frequency spectrum. However frequency based approaches rely on good linear approximations.

Other ego-motion estimation coupled approaches are often based on Kalman filters, where the parameters are added to the filter state. The work presented in [11] offers a comparison of common methods for doing this estimation, and compares EKF, simplified unscented Kalman filter (UKF), and full UKF for estimating various non-linear aerodynamic effects on both fixed-wing and coaxial helicopter platforms. In contrast to our work, they do not take the raw IMU measurements into account.

Another big field for on-line parameter estimation is adaptive control, where the parameter estimation is closely tied to the control. Estimating the inertia as an example was first developed for general rigid bodies [12] and applied to MAVs in [13]. Other work is based on recursive least squares as shown in [14] where the unknown mass was estimated.

In this paper we extend our previous work [15], where we estimate the dominant parameters of the MAV in a batch maximum likelihood (ML) estimator. We combined measurements from the IMU, the MAV dynamic model driven by the motor speeds, and external tracking system to take all available information into account. With our new algorithm we are able to include all this measurements in a filter-based approach and estimate the parameters in real time.

III. Generalized Information Filtering

In many robotic applications there is a trend towards an increasing number of sensors and models that need to be combined into a single concise state estimation process. A classical approach is to employ an EKF. However, this imposes many restrictions on the set of models that can be used. Various extensions exist to handle special cases such as correlated noise between prediction and update phase.

Therefore, when it comes to complex systems, it is often simpler to represent the maximum likelihood estimation problem with the aid of factor graphs or error terms and solve it in an incremental or batch fashion. In this section we derive a general filtering algorithm, from now on referred to as generalized information filter (GIF), which can be applied to a wider set of sensor fusion problems than the regular EKF. The derivation is based on the maximum likelihood estimation that can be associated with every KF [16]. Our generalized set of filtering equations result from a slightly adapted maximum likelihood problem.

A. Optimization Based Filtering

For better understandability most equations are derived by considering the linear case. The extension to non-linear cases is analogous to the relation between regular KF and EKF [2]. The negative log-likelihood form of the MLE optimization problem that leads to the regular KF equations can be written as:

$$
\begin{aligned}
L(\boldsymbol{x}_k^k, \boldsymbol{x}_{k-1}^k) &= \|\boldsymbol{x}_{k-1}^k - \boldsymbol{x}_{k-1}^{k-1}\|^2_{\boldsymbol{P}_{k-1}^{-1}} && (1)\\
&+ \|\boldsymbol{x}_k^k - \boldsymbol{F}\boldsymbol{x}_{k-1}^k - \boldsymbol{G}\boldsymbol{u}_{k-1}\|^2_{\boldsymbol{Q}^{-1}} && (2)\\
&+ \|\boldsymbol{z}_k - \boldsymbol{H}\boldsymbol{x}_k^k - \boldsymbol{v}_k\|^2_{\boldsymbol{R}^{-1}}. && (3)
\end{aligned}
$$

In the above equation we employ the notation where $\boldsymbol{x}_k^m$ represents the estimated state at timestep k when including all information up to time step m. E.g., $\boldsymbol{x}_{k-1}^k$ represents the estimated state at time $k-1$ when integrating all information up to time step k. The matrices, $\boldsymbol{F}, \boldsymbol{G}, \boldsymbol{Q}, \boldsymbol{H}, \boldsymbol{R}$ describe the stochastic system, and the vectors $\boldsymbol{u}$ and $\boldsymbol{z}$ are the process input and the update measurement, respectively.

We propose the use of a fully implicit formulation of the estimation problem and rely on the concept of residuals rather than on the paradigm of process and measurement models. Compared to the above optimization problem, we merge the prediction (2) and update (3) into a single stacked linear residual

$$
\boldsymbol{r}_k = \boldsymbol{A}\boldsymbol{x}_k^k + \boldsymbol{B}\boldsymbol{x}_{k-1}^k + \boldsymbol{b}_k. \tag{4}
$$

Together with the prior (1), this yields the following negative log-likelihood cost function:

$$
\begin{aligned}
L(\boldsymbol{x}_k^k, \boldsymbol{x}_{k-1}^k) &= \|\boldsymbol{x}_{k-1}^k - \boldsymbol{x}_{k-1}^{k-1}\|^2_{\boldsymbol{P}_{k-1}^{-1}} && (5)\\
&+ \|\boldsymbol{A}\boldsymbol{x}_k^k + \boldsymbol{B}\boldsymbol{x}_{k-1}^k + \boldsymbol{b}_k\|^2_{\boldsymbol{W}^{-1}}. && (6)
\end{aligned}
$$

One can also verify that the original problem can be retrieved as special case of this form, where the matrices are selected as:

$$\boldsymbol{A} = \begin{bmatrix} \boldsymbol{I} \\ -\boldsymbol{H} \end{bmatrix}, \boldsymbol{B} \quad = \quad \begin{bmatrix} -\boldsymbol{F} \\ \boldsymbol{0} \end{bmatrix}, \boldsymbol{b}_k = \begin{bmatrix} -\boldsymbol{G}\boldsymbol{u}_{k-1} \\ \boldsymbol{z}_k - \boldsymbol{v}_k \end{bmatrix},$$
$$\boldsymbol{W} \quad = \quad \begin{bmatrix} \boldsymbol{Q} & 0 \\ 0 & \boldsymbol{R} \end{bmatrix}$$

While we can do regular KF with the presented form, much more general system models can be integrated in this manner. For instance correlated noise between prediction and update step can easily be considered by adapting the off-diagonal terms of the joint covariance matrix $\boldsymbol{W}$. Also, multiple or even missing prediction models can be inherently handled by adding or removing residuals. In certain cases this can strongly simplify the design and implementation of KFs.

B. Recursive Algorithm

Analogously to the regular Kalman filter, a set of recursive equations can be derived. Among different possible forms, we chose an information matrix based formulation which tracks the information matrix $\boldsymbol{Y}_k = \boldsymbol{P}_k^{-1}$ instead of the covariance matrix itself. In contrast to most work on information filtering we recover the state at every time step, since we need it for the linearization point. This enables us to derive a compact and efficient algorithm.

Given a prior distribution on the previous state $(\boldsymbol{x}_{k-1}^{k-1}, \boldsymbol{Y}_{k-1})$, the recursive equations provide an estimate for the current state $(\boldsymbol{x}_k^k, \boldsymbol{Y}_k)$ while integrating all measurements/information up to time step k:

$$\boldsymbol{D}_k = \boldsymbol{Y}_{k-1} + \boldsymbol{B}^T\boldsymbol{W}^{-1}\boldsymbol{B} \tag{7}$$
$$\boldsymbol{S}_k = \boldsymbol{A}^T\boldsymbol{W}^{-1}(\boldsymbol{I} - \boldsymbol{B}\boldsymbol{D}_k^{-1}\boldsymbol{B}^T\boldsymbol{W}^{-1}) \tag{8}$$
$$\boldsymbol{Y}_k^k = \boldsymbol{S}_k\boldsymbol{A} \tag{9}$$
$$\boldsymbol{Y}_k\boldsymbol{x}_k^k = -\boldsymbol{S}_k\left(\boldsymbol{B}\boldsymbol{x}_{k-1}^{k-1} + \boldsymbol{b}_k\right). \tag{10}$$

The last equation represents the solving of a linear system and the full setup requires only one matrix inversion (assuming that $\boldsymbol{W}^{-1}$ can be pre-computed). Independent of the number of update measurements, the inversion always involves a $n \times n$ matrix, where n is the dimension of the filter state. The derivation of the above filter equations can be obtained by setting the differentials of the log-likelihood w.r.t. both states, $\boldsymbol{x}_{k-1}^{k-1}$ and $\boldsymbol{x}_k^k$, to zero and employing linear algebra (we omit the full derivation here due to space restrictions).

C. Extension to Nonlinear Systems

In the case of nonlinear systems the selection of linearization points, $\bar{\boldsymbol{x}}_k^k$ and $\bar{\boldsymbol{x}}_{k-1}^k$, is required around which Jacobians are evaluated. These Jacobians are then used to construct the filtering matrices $\boldsymbol{A}$, $\boldsymbol{B}$, $\boldsymbol{W}$ and the vector $\boldsymbol{b}_k$. The nonlinear residual $\boldsymbol{r}_k = \boldsymbol{f}(\boldsymbol{x}_k^k, \boldsymbol{x}_{k-1}^k)$, which directly integrates all measurements, is approximated by:

$$\boldsymbol{r}_k \approx \boldsymbol{A}_k\Delta\boldsymbol{x}_k^k + \boldsymbol{B}_k\Delta\boldsymbol{x}_{k-1}^k + \boldsymbol{b}_k, \tag{11}$$

with $\Delta\boldsymbol{x}_{k-1}^k = \boldsymbol{x}_{k-1}^k - \bar{\boldsymbol{x}}_{k-1}^k$, $\Delta\boldsymbol{x}_k^k = \boldsymbol{x}_k^k - \bar{\boldsymbol{x}}_k^k$ and

$$\boldsymbol{A}_k = \frac{\partial \boldsymbol{f}}{\partial \boldsymbol{x}_k^k}(\bar{\boldsymbol{x}}_{k-1}^k, \bar{\boldsymbol{x}}_k^k) \tag{12}$$
$$\boldsymbol{B}_k = \frac{\partial \boldsymbol{f}}{\partial \boldsymbol{x}_{k-1}^k}(\bar{\boldsymbol{x}}_{k-1}^k, \bar{\boldsymbol{x}}_k^k)$$
$$\boldsymbol{b}_k = \boldsymbol{f}(\bar{\boldsymbol{x}}_{k-1}^k, \bar{\boldsymbol{x}}_k^k).$$

While $\bar{\boldsymbol{x}}_{k-1}^k$ can be chosen to be equal to the prior on the previous state $\boldsymbol{x}_{k-1}^{k-1}$, the choice for $\bar{\boldsymbol{x}}_k^k$ is non-trivial. Often, however, some good guess is available through some motion model.

The main advantage of this formulation is that arbitrary measurements can be included into the filter as long as they can be represented as function of two subsequent filter states. On-the-fly enabling and disabling of certain measurements quantities can be achieved by just removing the corresponding sections of the filtering matrices. Also, similarly to the iterated EKF [16], an iterative scheme can be applied to achieve higher accuracy at the cost of an increased computational effort.

IV. Model Description

We validate our new formulation on two different models. First, we demonstrate in detail how the new recursive formulation of the filter may be applied, through the use of a simple example involving a 1D MAV model. Second, we present the full MAV model of the hexacopter used in our experiments.

A. Simple 1D MAV Modelling

By only considering the z direction of an MAV we can derive a very simplistic 1D MAV model which is shown in Fig. 2. We want to estimate the position, velocity and the unknown thrust coefficient c_T that maps the input u of the motors to the produced force.

This leads to the following discrete time equations:

$$p_k = p_{k-1} + v_{k-1}\Delta t + w_{p,k-1} \tag{13}$$
$$v_k = v_{k-1} + \frac{\Delta t}{m} c_{T,k-1}\left(u_{k-1} + w_{u,k-1}\right) - g\,\Delta t$$
$$c_{T,k} = c_{T,k-1} + w_{c,k-1}$$

where g is the gravity acceleration and $w_{*,k} \sim \mathcal{N}(0, Q_*)$ Gaussian noise. For the example, we assume the availability of a position measurement

$$\tilde{p}_k = p_k + w_{\tilde{p},k}, \quad w_{\tilde{p},k} \sim \mathcal{N}(0, Q_{\tilde{p}}) \tag{14}$$

and the accelerometer measurement

$$\tilde{a}_k = a_k + g + w_{\tilde{a},k}, \quad w_{\tilde{a},k} \sim \mathcal{N}(0, Q_{\tilde{a}}) \tag{15}$$

where a_k is the acceleration of the center of gravity (CoG) of the MAV at time k. The accelerometer measurement can be considered an alternative prediction model for the velocity of the MAV which is common in many applications:

$$v_k = v_{k-1} + \left(\tilde{a}_{k-1} - w_{\tilde{a},k-1} - g\right)\Delta t \tag{16}$$

to which we refer as the IMU model.

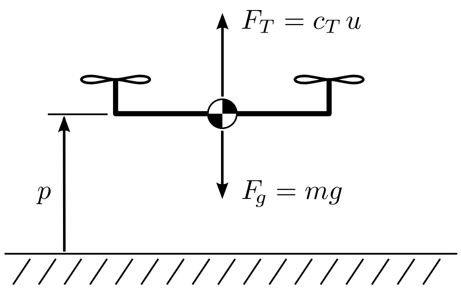

Fig. 2. A schematically depicted 1D MAV that can only move in z direction. We measure the position with a height sensor. Furthermore we know the force generated by the motors and we have an IMU that measures acceleration in z.

We use these simple equations to demonstrate the modeling and the estimation performance of our new filter approach. For comparison, we implemented an EKF using the dynamic model (13) and the position measurement, and a state-augmented EKF formulation (A-EKF). For the A-EKF, a full kinematic model similar to (16) is augmented with the MAV's acceleration and a constant acceleration model:

$$a_k \;=\; a_{k-1} + w_{a,k-1}, \quad w_{a,k-1} \sim \mathcal{N}(0, Q_a) \quad (17)$$

The state augmentation allows the formulation of an innovation residual that exploits both, the IMU and the dynamic model:

$$\boldsymbol{z}_k - \boldsymbol{h}(\boldsymbol{x}_k, u_k) = \begin{bmatrix} \tilde{p}_k \\ \tilde{a}_k \\ 0 \end{bmatrix} - \begin{bmatrix} p_k \\ g + a_k \\ a_k - \left(\frac{1}{m} c_{T,k}\, u_k - g\right) \end{bmatrix} \quad . \; (18)$$

Our filter formulation circumvents the state augmentation by directly formulating the predictions and measurements equations as residuals of the negative log-likelihood function. If we choose the linearization points $\bar{\boldsymbol{x}}_{k-1}^{k} = \begin{bmatrix} p_{k-1}^{k-1} & v_{k-1}^{k-1} & c_{T,k-1}^{k-1} \end{bmatrix}$ and $\bar{\boldsymbol{x}}_k^k$ as, e.g., the prediction from (13), we find the following $\boldsymbol{A}_k$, $\boldsymbol{B}_k$, $\boldsymbol{b}_k$, $\boldsymbol{W}_k$ matrices:

$$\boldsymbol{A}_k = \begin{bmatrix} 1 & 0 & 0 \\ 0 & 1 & 0 \\ 0 & 0 & 1 \\ 0 & 1 & 0 \\ -1 & 0 & 0 \end{bmatrix}, \boldsymbol{B}_k = \begin{bmatrix} -1 & -\Delta t & 0 \\ 0 & -1 & -\frac{\Delta t}{m} u_{k-1} \\ 0 & 0 & -1 \\ 0 & -1 & 0 \\ 0 & 0 & 0 \end{bmatrix},$$

$$\boldsymbol{b}_k = \begin{bmatrix} \bar{p}_k^k - \left(\bar{p}_{k-1}^k + \bar{v}_{k-1}^k \Delta t\right) \\ \bar{v}_k^k - \left(\bar{v}_{k-1}^k + \frac{\Delta t}{m} \bar{c}_{T,k-1}^k u_{k-1} - g\,\Delta t\right) \\ \bar{c}_{T,k}^k - \bar{c}_{T,k-1}^k \\ \bar{v}_k^k - \left(\bar{v}_{k-1}^k + (\tilde{a}_{k-1} - g)\,\Delta t\right) \\ \tilde{p}_k - \bar{p}_k^k \end{bmatrix},$$

$$\boldsymbol{W}_k = \operatorname{diag}\begin{bmatrix} Q_r & (\frac{\Delta t}{m} c_{T,k-1})^2 Q_u & Q_{c_T} & \Delta t^2 Q_{\tilde{a}} & Q_{\tilde{p}} \end{bmatrix}$$

where the top three rows include the dynamic model residual, the fourth row includes the IMU model residual, and the last row includes the noisy height measurement.

B. Full MAV Model

For MAV multirotor helicopters equipped with an onboard IMU, two process models are available. One is the MAV dynamical model, driven by the motor speeds and the forces and moments they induce. In addition to this, the IMU provides an additional source of information, which can be used to estimate their motion.

In a classical filtering approach we would need to augment the state vector with the acceleration to incorporate the two motion models in the update phase of the filter and make some assumption about the evolution of the acceleration. This is not needed with our new algorithm.

We make the following two assumptions to simplify the dynamic equations. The CoG of the MAV coincides with the center of the main body and the motors are all aligned with the MAVs z-axis.

On our experimental platform the above assumptions do not hold and we use a more complete model in our implementation for the final results, which is described in our previous work [15]. These extensions are not important for the operation and understanding of the proposed filtering strategy and are omitted to simplify the equations.

1) Forces and Moments Acting on the MAV: The MAV dynamic model is driven by the measured motor speeds $\tilde{\boldsymbol{n}}_k$, which are modeled as follows:

$$\tilde{\boldsymbol{n}}_k = \boldsymbol{n}_k + \mathbf{w}_v \quad (19)$$

where $\mathbf{w}_v$ denotes a zero mean, discrete-time Gaussian noise with variance $\mathbf{Q}_v$.

The forces acting on the rotor hub of every rotor i are given by:

$$_B\boldsymbol{F}_i \;=\; \left(\boldsymbol{T}_i - T_i c_{dB} \boldsymbol{v}_{hub,i}^{\perp}\right) + \mathbf{w}_F \quad (20)$$

$$T_i \;=\; c_T \tilde{n}_i^2;\; \boldsymbol{T}_i = T_i \boldsymbol{e}_z. \quad (21)$$

where we again add normally distributed noise $\mathbf{w}_F$ to account for aerodynamic uncertainties. The thrust T_i is given by the multiplication of the squared rotor speed and the thrust coefficient c_T. We also introduce the combined drag coefficient c_d, to account for the induced drag and blade flapping [17]. The vector $_B\boldsymbol{v}_{hub,i}^{\perp}$ denotes the projected linear velocity of the rotor hub i onto the rotor plane and is given by

$$_B\boldsymbol{v}_{hub,i}^{\perp} = \begin{bmatrix} 1 & 0 & 0 \\ 0 & 1 & 0 \\ 0 & 0 & 0 \end{bmatrix} ({}_B\boldsymbol{v} + {}_B\boldsymbol{\omega} \times {}_B\boldsymbol{r}_{BA_i}), \quad (22)$$

where $_B\boldsymbol{r}_{BA_i}$ denotes the offset of the rotor hub from the IMU, $_B\boldsymbol{v}$ the velocity of the MAV and $_B\boldsymbol{\omega}$ the angular rates, both expressed in body coordinates.

This leads to the total force produced by the motors $_B\boldsymbol{F}_{tot}$:

$$_B\boldsymbol{F}_{tot} = \sum_{i=1}^{6} {}_B\boldsymbol{F}_i. \quad (23)$$

The total moment around the CoG is given by:

$$_B\boldsymbol{M}_{tot} \;=\; \sum_{i=1}^{6} (\boldsymbol{M}_i + {}_B\boldsymbol{F}_i \times {}_B\boldsymbol{r}_{BA_i}) + \mathbf{w}_M \quad (24)$$

$$\boldsymbol{M}_i \;=\; c_m \tilde{n}_i^2 \boldsymbol{e}_z, \quad (25)$$

with the normally distributed process noise $\mathbf{w}_M$ to account for aerodynamic uncertainties. Here we introduced the moment coefficient c_m relating the rotational velocity of the propeller to the produced moment.

2) MAV Dynamic Model: We assume that the inertia matrix J is diagonal and fixed the inertia J_{zz} to the measured value, since it has very similar effect on the system as the moment coefficient c_m and is very hard to estimate. For the MAV model we stack all the parameters into one parameter vector $\boldsymbol{\theta} = [c_T, c_m, c_d, J_{xx}, J_{yy}]$, that we append to the state for the estimation. We also add normally distributed process noise to all parameters $\mathbf{w}_\theta$. This leads to the final MAV model driven by the measured motor speeds $\tilde{\boldsymbol{n}}$.

$$
\begin{aligned}
{}_I\dot{\boldsymbol{r}}_{IB} &= \boldsymbol{C}_{IB\,B}\boldsymbol{v}_B \qquad (26)\\
{}_B\dot{\boldsymbol{v}}_B &= \frac{1}{m}\,{}_B\boldsymbol{F}_{tot} - \boldsymbol{C}_{IB}^T \cdot {}_I\boldsymbol{g} - \boldsymbol{\omega} \times {}_B\boldsymbol{v}_B\\
\dot{\boldsymbol{q}}_{IB} &= \frac{1}{2}\Omega(\boldsymbol{\omega})\,\boldsymbol{q}_{IB}\\
\dot{\boldsymbol{\omega}} &= \boldsymbol{J}^{-1}\left({}_B\boldsymbol{M}_{tot} - \boldsymbol{\omega} \times \boldsymbol{J}\boldsymbol{\omega}\right)\\
\dot{\boldsymbol{\theta}} &= \mathbf{w}_\theta
\end{aligned}
$$

with

$$
\boldsymbol{\Omega}(\boldsymbol{\omega}) = \begin{bmatrix} 0 & -\boldsymbol{\omega}^T \\ \boldsymbol{\omega} & -[\boldsymbol{\omega}]_\times \end{bmatrix}.
$$

3) IMU Model: We model the IMU measurements with additive white Gaussian noise and a slowly varying bias process:

$$
\begin{aligned}
\tilde{\boldsymbol{a}} &= \boldsymbol{a} + \mathbf{b}_a + \mathbf{w}_a \qquad (27)\\
\tilde{\boldsymbol{\omega}} &= \boldsymbol{\omega} + \mathbf{b}_w + \mathbf{w}_w,
\end{aligned}
$$

where $\tilde{\boldsymbol{a}}$ denotes the accelerometer and $\tilde{\boldsymbol{\omega}}$ the gyroscope measurements corrupted with Gaussian white noise processes $\mathbf{w}_a$ and $\mathbf{w}_w$ of strength $\sigma_a^2\mathbf{I}$ and $\sigma_w^2\mathbf{I}$. Random walk processes $\mathbf{b}_a$ and $\mathbf{b}_w$ with diffusion $\sigma_{ba}\mathbf{I}$ and $\sigma_{bw}\mathbf{I}$ model the accelerometer and gyroscope bias processes.

This leads to the following IMU-driven process model:

$$
\begin{aligned}
{}_B\dot{\boldsymbol{v}}_B &= \tilde{\boldsymbol{a}} - \mathbf{b}_a - \mathbf{w}_a - \boldsymbol{C}_{IB}^T{}_I\boldsymbol{g} \qquad (28)\\
&\quad -(\tilde{\boldsymbol{\omega}} - \mathbf{b}_w - \mathbf{w}_w) \times {}_B\boldsymbol{v}_B \qquad (29)\\
\dot{\boldsymbol{q}}_{IB} &= \frac{1}{2}\Omega(\tilde{\boldsymbol{\omega}} - \mathbf{b}_w - \mathbf{w}_w)\,\boldsymbol{q}_{IB} \qquad (30)\\
\dot{\mathbf{b}}_w &= \mathbf{w}_{b_w} \qquad (31)\\
\dot{\mathbf{b}}_a &= \mathbf{w}_{b_a} \qquad (32)
\end{aligned}
$$

4) Position and Attitude Measurements: We use a motion tracking system[1] to obtain position and attitude measurements of the MAV. The measurements are modeled as follows:

$$
\begin{aligned}
\tilde{\boldsymbol{p}}_k &= {}_I\boldsymbol{p}_{B,k} + \mathbf{w}_{p,k} \qquad (33)\\
\tilde{\boldsymbol{q}}_k &= \boldsymbol{q}_{IB,k} \otimes \mathbf{q}_{q,k}, \qquad (34)
\end{aligned}
$$

where $\mathbf{w}_{p,k}$ denotes additive discrete Gaussian noise with covariance $\mathbf{R}_p$, $\mathbf{w}_{p,k} \sim \mathcal{N}(\mathbf{0}, \mathbf{R}_p)$ and where $\mathbf{q}_{q,k}$ describes rotational noise with normally distributed small angles, $\mathbf{q}_{q,k} \approx \begin{bmatrix} \frac{1}{2}\mathbf{w}_{\phi,k}^T & 1 \end{bmatrix}^T$ with $\mathbf{w}_{\phi,k} \sim \mathcal{N}(\mathbf{0}, \mathbf{R}_q)$.

[1] http://www.vicon.com/products/camera-systems/bonita

5) Filter Design: To formulate an EKF and our new GIF with both process models we define the state as

$$
\boldsymbol{x} = [{}_I\boldsymbol{r}_{IB}, {}_B\boldsymbol{v}_B, \boldsymbol{q}_{IB}, \boldsymbol{\omega}, \mathbf{b}_w, \mathbf{b}_a, \boldsymbol{\theta}]\,. \qquad (35)
$$

The two previously defined process models equation (26) and (28) can now be discretized and expressed as a function of the state $\boldsymbol{x}_k = \boldsymbol{f}_{MAV,d}(\boldsymbol{x}_{k-1})$ and $\boldsymbol{x}_k = \boldsymbol{f}_{IMU,d}(\boldsymbol{x}_{k-1})$. Similar to the process models we define the discrete position and attitude measurement function from (33) as $\boldsymbol{h}(\boldsymbol{x}_k)$. From this we are able to formulate the nonlinear residual functions and calculate the necessary Jacobians for our GIF as described in (11).

$$
\begin{aligned}
\boldsymbol{r}_{MAV} &= \boldsymbol{x}_k - \boldsymbol{f}_{MAV,d}(\boldsymbol{x}_{k-1}) \qquad (36)\\
\boldsymbol{r}_{IMU} &= \boldsymbol{x}_k - \boldsymbol{f}_{IMU,d}(\boldsymbol{x}_{k-1}) \qquad (37)\\
\boldsymbol{r}_z &= \boldsymbol{z}_k - \boldsymbol{h}(\boldsymbol{x}_k) \qquad (38)
\end{aligned}
$$

V. Results

We first validate the new formulation on a simple simulation example with exact ground truth. Then, in a second part we apply the generalized information filtering to the problem of parameter estimation for our MAV and give some deeper insight on the advantages and limitations of the new formulation.

A. Simulation Results on 1D MAV

To analyze the properties of the new formulation in detail, we show a simple 1D MAV simulation in z-direction. This allows easier comparisons of different approaches to estimate the trajectory and parameters. We additionally try to highlight the advantages and disadvantages of the new formulation.

Fig. 3 depicts the estimation error for the position and thrust coefficient of the system. Two main observations can be highlighted. Firstly, the augmented EKF (A-EKF) and the proposed GIF both exhibit faster convergence for the parameter estimation (thrust coefficient) than the regular EKF which neglects the acceleration information. This can be attributed to the additional use of IMU-data which improves the estimation of quantities involved in the dynamic model (velocities/accelerations) and thus provides a stronger feedback on the estimation of the thrust coefficient. On the other hand the estimation of the pose is comparable for all three estimators.

Secondly, the proposed GIF does not suffer from any inconsistencies related to inclusion of additional and erroneous priors. This can be observed for the A-EKF, which due to its smooth acceleration prior exhibits inconsistencies once a significant change in acceleration occurs at 5 s (the error falls out of the estimated σ-bounds). This demonstrates that the presented GIF can include multiple process models without relying on additional, potentially erroneous, priors.

B. Experimental Validation

For our experimental validation we recorded short manual flights and recorded the position of the MAV with a Vicon tracking system. During this trajectory, all axes of the MAV

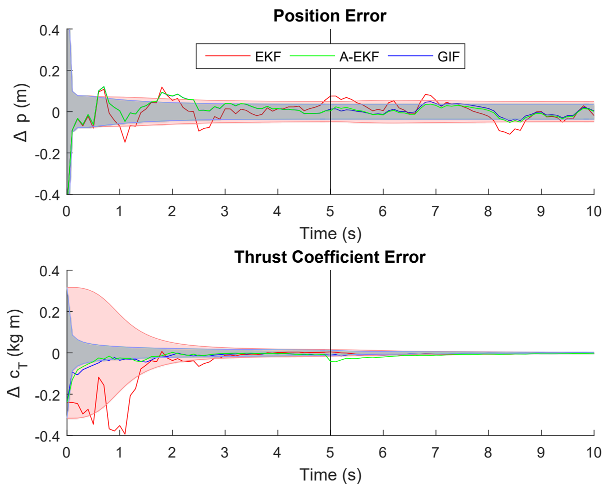

Fig. 3. Estimation errors for position and thrust coefficient for a simple 1D MAV model. Three filter setups are compared: two EKF setups (regular without IMU, and augmented with acceleration state to include the IMU) and the proposed GIF framework. The dotted lines depict the estimated σ-bounds (they mostly lie over each other for the A-EKF and GIF). While overall the trajectory exhibits smooth accelerations, there is a significant acceleration step change at 5s. Since the augmented EKF relies on a smooth acceleration prior it gets strongly affected by the step change. The regular EKF without IMU-data exhibits a slower convergence rate for the thrust coefficient.

were excited to maximize the observability of the unknown parameters.

We compare our new GIF algorithm to a standard parameter estimation EKF (neglecting IMU data), as well as to results from a batch optimization which serves as ground truth. Since all Jacobians are already derived in our GIF framework they are directly used in the EKF implementation with the same noise properties. The external motion tracking system provides very accurate motion estimates such that including IMU data does not have a strong influence on the parameter estimation. Thus, although the EKF does not include IMU data, it provides a good reference in terms of parameter estimation and allows to analyze the advantages and limitations of our approach.

In Fig. 4 the estimated aerodynamic coefficients are shown together with the 1σ bounds. Ground truth for the aerodynamic coefficients is estimated in a batch maximum likelihood optimization described in our previous work [15]. The performance of both estimators is very similar and only differs in the first few time steps where the GIF converges faster. This is especially true for the thrust coefficient (c_T), that in the GIF converges to a value close to the final solution in only one time step. Also, note that the thrust coefficient is not truly constant over the entire trajectory depending on the MAV's velocity and angle as is described in [18]. Unlike the other aerodynamic coefficients, the moment coefficient (c_m) exhibits very slow convergence. This is due to the limited motion around the yaw axis that the MAV undergoes during its trajectory.

The estimated inertia parameters with standard Vicon estimates and when the Vicon has had the noise in its attitude estimates artificially increased to $\sigma = 0.5^\circ$ are shown in Fig.

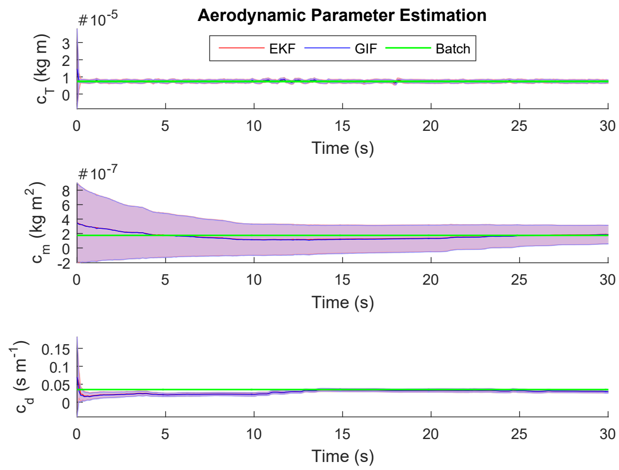

Fig. 4. Estimated aerodynamic coefficients with an EKF and our new formulation that also includes IMU measurements. Except for the moment coefficient, the parameters converge very quickly. Adding the IMU mainly helps the thrust constant, which converges immediately. The moment coefficient is the only parameter that exhibits significant uncertainty after the flight.

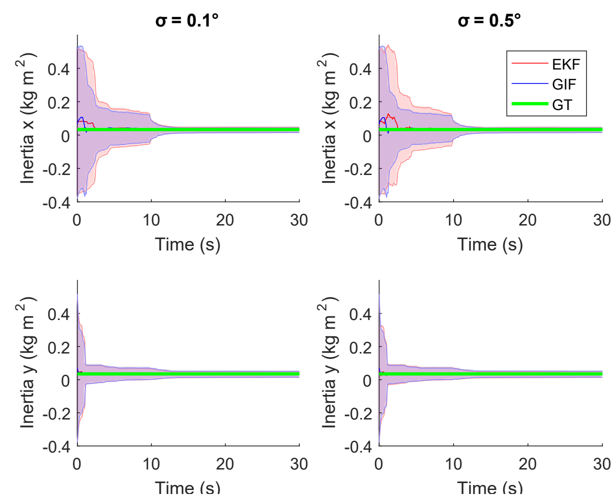

Fig. 5. Estimated Inertia in x and y direction for two different noise levels in the attitude estimation. The plots on the left show the process run utilizing the Vicon pose estimates. Due to the high accuracy of the Vicon information there is no significant difference in estimating the parameters in an EKF or adding the IMU to the estimation process. The plots on the right show the process with increased noise in the Vicon system. Adding the information provided by the IMU in this situation increases the convergence rate.

5. On the left section of the figure, we show the estimated parameters without additional noise on the Vicon. Since the noise on the Vicon measurements is small, there is almost no benefit in using the IMU for the parameter estimation. However, in cases where the quality of the pose estimate the Vicon provides decreases the convergence rate of the EKF also decreases. In these same conditions in the GIF framework, the IMU information gains more weight. This leads to GIF giving results that are comparable with the no additional noise case. This behavior can be of significant benefit in the context of on-board parameter estimation, where the pose must be provided by methods such as visual-inertia odometry. The pose estimates of these methods are

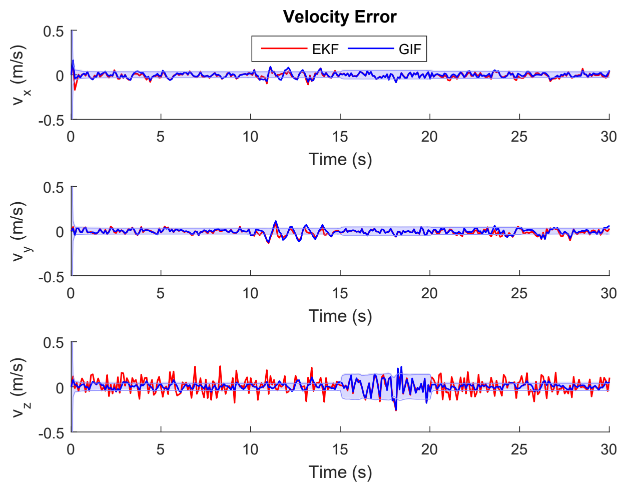

Fig. 6. Velocity error of the GIF state under gaussian measurement noise of 1 cm standart deviation on position. To show the benefit of the new formulation we disable individual sensors. The IMU is disabled for 5 s at the 15 s mark. After this the MAV model is disabled for 5s starting at the 20 s mark.

likely to be of significantly worse quality than that provided by a Vicon system.

A useful property of the new formulation is that similar to the Kalman filter, where individual measurement updates can be dropped, it is possible to turn off one of the process models without changing the structure of the filter. This can be done as all the states and covariances are still tracked without any additional work on the filter. This property makes the filter ideal for adding fail safety to a system in case of sudden sensor drop out. We demonstrate this fail safety property in a final experiment shown in Fig. 6. In this experiment we simulate a failure of the IMU by discarding its measurements for 5 s starting at the 15 s mark. As expected the behavior of our new filter is almost identical to the EKF without the IMU during that period, since the parameters converged for both filters to similar values after this time. At the 20 s mark we re-enable the IMU and disable the MAV dynamic model for 5 s. Again, the filter handles this change in sensor outputs. However, in this case the effects of dropping the dynamic model are very small compared to the effect of the dropping the IMU. This leads us to the conclusion that in this instance, for our system, while the model can provide robustness against IMU failure, it is not accurate enough to replace the IMU.

VI. Conclusion

In this paper we have presented a generalized information filter that is capable of handling multiple system and measurement models simultaneously. The presented formulation is very general and applicable to a broad variety of problems, where models might even involve correlated noise. In robotics, for instance, the use of multiple process models may be desirable to simultaneously consider a dynamical model and an IMU-driven model in the prediction step.

Our scenario considers this situation for the case of MAVs. It is shown that, compared to a classical EKF, the entire recursive estimator can be simplified as it is not necessary to augment the state with additional linear and angular acceleration states. In simulation and real-world experiments, we validate the functionality and flexibility of the proposed estimator. It is also shown how in the considered scenario, the proposed approach converges faster in comparison to the EKF.

References

[1] R. E. Kalman, "A New Approach to Linear Filtering and Prediction Problems," *Journal of Basic Engineering*, vol. 82, no. 1, p. 35, mar 1960.

[2] G. L. Smith, S. F. Schmidt, and L. A. McGee, "Application of Statistical Filter Theory to the Optimal Estimation of Position and Velocity on Board a Circumlunar Vehicle," National Aeronautics and Space Administration (NASA), Tech. Rep., 1962.

[3] H. Blom and Y. Bar-Shalom, "The interacting multiple model algorithm for systems with Markovian switching coefficients," *IEEE Transactions on Automatic Control*, vol. 33, no. 8, pp. 780–783, 1988.

[4] Y. Bar-Shalom and L. Campo, "The Effect of the Common Process Noise on the Two-Sensor Fused-Track Covariance," *IEEE Transactions on Aerospace and Electronic Systems*, vol. AES-22, no. 6, pp. 803–805, nov 1986.

[5] S. Grime and H. Durrant-Whyte, "Data fusion in decentralized sensor networks," *Control Engineering Practice*, vol. 2, no. 5, pp. 849–863, oct 1994.

[6] K. Chang, R. Saha, and Y. Bar-Shalom, "On optimal track-to-track fusion," *IEEE Transactions on Aerospace and Electronic Systems*, vol. 33, no. 4, pp. 1271–1276, oct 1997.

[7] Ting Yuan, Y. Bar-Shalom, and Xin Tian, "Heterogeneous track-to-track fusion," in *Proceedings of the 14th International Conference on Information Fusion (FUSION)*, 2011, pp. 1–8.

[8] M. Skliar and W. F. Ramirez, "Implicit Kalman filtering." *International journal of control*, vol. 66, no. 3, pp. 393–412, jan 1997.

[9] R. Steffen, "A Robust Iterative Kalman Filter Based on Implicit Measurement Equations," *Photogrammetrie - Fernerkundung - Geoinformation*, vol. 2013, no. 4, pp. 323–332, aug 2013.

[10] E. A. Morelli, "Real-time parameter estimation in the frequency domain," *Journal of Guidance, Control, and Dynamics*, vol. 23, no. 5, pp. 812–818, 2000.

[11] G. Chowdhary and R. Jategaonkar, "Aerodynamic parameter estimation from flight data applying extended and unscented kalman filter," *Aerospace science and technology*, vol. 14, no. 2, pp. 106–117, 2010.

[12] N. A. Chaturvedi, D. S. Bernstein, J. Ahmed, F. Bacconi, and N. H. McClamroch, "Globally convergent adaptive tracking of angular velocity and inertia identification for a 3-dof rigid body," *Control Systems Technology, IEEE Transactions on*, vol. 14, no. 5, pp. 841–853, 2006.

[13] M. I. Rashid and S. Akhtar, "Adaptive control of a quadrotor with unknown model parameters," in *Applied Sciences and Technology (IBCAST), 2012 9th International Bhurban Conference on*. IEEE, 2012, pp. 8–14.

[14] D. Mellinger, Q. Lindsey, M. Shomin, and V. Kumar, "Design, modeling, estimation and control for aerial grasping and manipulation," in *Intelligent Robots and Systems (IROS), 2011 IEEE/RSJ International Conference on*. IEEE, 2011, pp. 2668–2673.

[15] M. Burri, J. Nikolic, H. Oleynikova, M. Achtelik W., and R. Siegwart, "Maximum likelihood parameter identification for mavs," in *Robotics and Automation (ICRA), 2016 IEEE International Conference on*. IEEE, 2016, p. to Appear.

[16] B. M. Bell and F. W. Cathey, "The iterated kalman filter update as a gauss-newton method," *IEEE Transactions on Automatic Control*, vol. 38, no. 2, pp. 294–297, 1993.

[17] R. Mahony, V. Kumar, and P. Corke, "Multirotor aerial vehicles: Modeling, estimation, and control of quadrotor," *Robotics & Automation Magazine, IEEE*, vol. 19, no. 3, pp. 20–32, 2012.

[18] H. Huang, G. M. Hoffmann, S. L. Waslander, and C. J. Tomlin, "Aerodynamics and control of autonomous quadrotor helicopters in aggressive maneuvering," in *Robotics and Automation, 2009. ICRA'09. IEEE International Conference on*. IEEE, 2009, pp. 3277–3282.